A Preliminary Light Analysis for EC19314-5915

A. Chen
Taipei Astronomical Museum
Email: alchen@tam.gov.tw

ABSTRACT

EC19314-5915 is an eclipsing nova-like variable star with an orbital period of 4.75 h. The intensive high-speed photometry was obtained in 1992 June and July. In addition to the flickering activity, its mean light curve shows a quasi-periodic oscillation with a period of 582 s. To analyze the eclipses, a programme was written to synthesize the light curves. A model with an optically thick steady-state disc was adopted to reconstruct the light curves. No satisfactory solutions were obtained in the calculations. Future high-speed photometry and time-resolved spectroscopy are required for future study

Keywords: binaries: eclipsing – stars: EC19314-5915 - cataclysmic variables

1. INTRODUCTION

Cataclysmic variables (CVs) are all semi-detached strongly interacting binary stars consisting of a Roche-lobe-filling red star (usually on or near the main sequence, the secondary) and a mass-accreting white dwarf (the primary). The strength of the magnetic field of the white dwarf plays a major role in governing the accretion of matter on to the white dwarf. If the magnetic field is not too strong then an accretion disc will form around the white dwarf. The structure and evolution of accretion discs can be studied in detail, with strong geometrical constraints in the case of eclipsing systems.

In 1989 March, EC19314-5915 was discovered as an ultraviolet excess (UVX) stellar objects in the Edinburgh-Cape Survey (Stobie et al. 1997). Buckley et al. (1992) reported that the object is a deeply eclipsing CV, which has an orbital period of 4.75 h. Its optical spectrum is unusual, compared to the known CVs. In addition to emission lines typical of CVs (Balmer, HeI and HeII), it shows metallic absorption lines. Buckley et al. (1992) suggested that these absorption features come from the third component in the system, a G-type dwarf contributing ~23 per cent of the light in B-band. The authors also argued that the system is possible a Z Cam dwarf nova. Based on the photometric and spectroscopic characteristics, it is very likely that the object is a nova-like variable (Chen 1994). In cataclysmic variables, two types of rapid oscillations generally appear in outbursting dwarf novae (DN) and nova-like variables (NLs): dwarf novae oscillations (DNO) and quasi-periodic oscillations (QPOs). Buckley et al. (1992) indicated that "there was no evidence for either dwarf nova oscillations or quasi-periodic oscillations". This is true from the inspection of the amplitude spectra of individual runs, because

the QPOs power is so weak and cannot be identified. In this paper, QPOs are detected in the "mean" light curve.

In addition to the study of the rapid light variations, the model fitting for the eclipses is presented. Because of deficiency of a faster computer, only few attempts were made to analyze the eclipses.

2. OBSERVATIONS

All the observations were obtained at the Sutherland site of the South African Astronomical Observatory during 1992 June-July. High-speed photometry (HSP) was made with the 0.75-m equipped with the University of Cape Town photometer (UCTP), of which are aperture photometers with offset guiding capability so that guiding corrections do not interrupt the programme star measurements. Each HSP run was obtained with 5s integrations in "white light" (i.e. no filter was used). Thus the effective wavelength and bandpass of the system were determined by the detector, a blue-sensitive, S-11, photomultiplier tube. Bearing in mind that CVs are ultraviolet-rich stars, the "white-light" measurements correspond to a "broad B" (called B_w) magnitude. A second photometer was used simultaneously with the UCTP in order to monitor the sky condition. A star in the neighbourhood of the programme star was randomly selected as a check star and was observed in the second photometer.

Sky background measurements were obtained at least every half an hour and subtracted from the star measurements by fitting a cubic spline to the sky data. The sky-subtracted data were then corrected for atmospheric extinction using extinction coefficients appropriate to Sutherland. Finally, the HSP data were reduced to zero mean and normalized by the mean intensity of the star during the run. Crude magnitudes of the star in the B_w band were obtained relative to blue E-region standard stars. Experience of this approach accumulated by us shows that systematic errors are about 0.1 mag. The observing log of HSP is listed in Table 1, which gives Run number, UT date, start HJD, duration, B_w, and peak-to-peak amplitude (ΔB_w).

Three HSP-runs (S5510, S5514 & S5519) were obtained under poor sky condition (such as thin cirrus and seeing change), the light loss was corrected from the second channel data using O'Donoghue's technique.

Table 1. Observing Log of High-Speed Photometry

Run	UT Date	Start HJD	Duration	Bw	ΔBw
	mm/dd/yr	2440000. +	(h)		
S5507	062592	8799.44600	4.0	13.5	1.3
S5510	062692	8800.33880	6.2	-	-
S5511	062792	8801.4456	3.6	13.5	1.4
S5514	062892	8802.3136	6.5	-	-
S5517	062992	8803.315	6.2	13.5	1.4
S5519	072992	8833.2342	6.0	-	-
S5521	073092	8834.2303	6.0	13.4	1.4

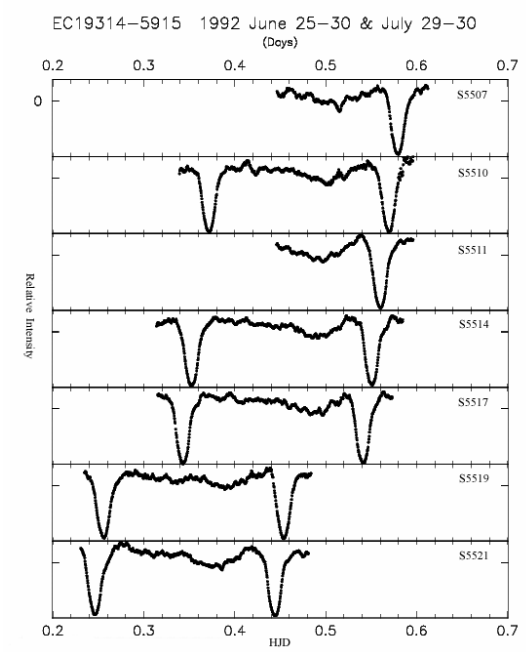

Fig. 1 The light curves for EC19314-5915 obtained in 1992 June and July.

3. PHOTOMETRIC CHARACTERISTICS

3.1 Times of Minimum Light for Eclipses

The HSP data in Table 1 are shown in Fig. 1. The light variation reveals low amplitude flickering and deep eclipses. The shape of the eclipses is obviously asymmetrical, which can be verified from Fig. 1. The eclipse depth is about 1.4 mag in white light, comparable to the depth 1.14 mag in B (Buckley et al. 1992). One may notice that there are two types of ingress, smooth ingress and steep ingress. The possible cause will be discussed in the next section.

An amplitude spectrum was calculated for the HSP data; its highest peak occurs at a frequency of 0.05848 mHz. In order to obtain the best estimate of the orbital period, another amplitude spectrum was calculated for the eclipse data (excluding the HSP data out of eclipse). The highest peak in the neighbourhood of 0.05848 mHz occurs at a frequency of 0.05841 mHz. For further search of the orbital period, a sinusoid of initial frequency 0.05841 mHz was fitted by non-linear least squares and gave a time of minimum light of 2448799.579521±0.000096, and an orbital period 0^d.198095±0.000006. One may argue that the above ephemeris may be incorrect due to the asymmetrical shape of the eclipses. Thus the middle line method (Ghedini 1982) was adopted to verify the above least squares method. This algorithm first defines middle points at brightnesses between minimum and maximum of eclipse and then a middle line was determined to give the point of minimum light. A rotation of the coordinates is required in order to correct for the asymmetric effect of light curve. Using the above algorithm, the times of the minimum light are estimated and listed in Table 2. A line was fitted by least squares and gave a time of minimum light of JD2448799.579574 and an orbital period 0^d.198098. The results are consistent with the previous calculations. We adopt JD2448799.579521 as the ephemeris for times of minimum light and 0^d.198095 as the

Table 2. Times of minimum light

Run	Cycle	Estimated Time HJD 2440000.+
S5507	0	8799.58013
S5510	4	8800.37169
	5	8800.57013
S5511	10	8801.56030
S5514	14	8802.35261
	15	8802.55108
S5517	19	8803.34352
	20	8803.54166
S5519	170	8833.25657
	171	8833.45330
S5521	175	8834.24693
	176	8834.44536

orbital period, because the standard deviations of the residuals for the least squares fit are smaller.

3.2 Search for Periodicity of Light Variation - Out of Eclipses

Outside eclipses, the light variation shows flickering activity with a peak-to-peak amplitude of ~0.35 Bmag, superposing on a hump modulation. The times of minimum light for the humps (marked arrows in Fig. 2) were determined by the visual inspection and are converted to orbital phases (Table 3). It shows the minimum light occurring at the orbital phases 0.65-0.78. This implies that the humps do not vary in phase with the orbital period. To investigate the possible periodicity for the hump modulation, a Fourier amplitude spectrum (Fig. 3) was calculated for the HSP data out of eclipses. The humps in the light curves do not vary sinusoidally, so alias patterns at both the hump period (P_{hp}) and the first harmonic of the hump period are visible in the amplitude spectrum. The amplitude spectrum shows a highest peak of 0.05841 mHz but other aliases are of similar amplitude. The diurnal aliases can be ruled out, because their frequencies are not double the prominent aliases in the first harmonic. Only three pairs of frequencies were found to be related by the expected 1:2 ratio. The possible values of P_{hp} are 3.9856, 3.4010, and 2.9775 hours and their first harmonics are 1.9933, 1.7008, and 1.4890 hours which are marked in Fig. 3. Among the above three peaks in Fig. 3, the amplitude of the 3.9856h-peak is stronger than that of the other two. Thus the period 3.9856h is the most likely alias to be the correct value of P_{hp}. This can be verified from the phases (see Table 3) of the minimum light of the humps corresponding to those three candidate periods.

In addition to the hump modulation, a

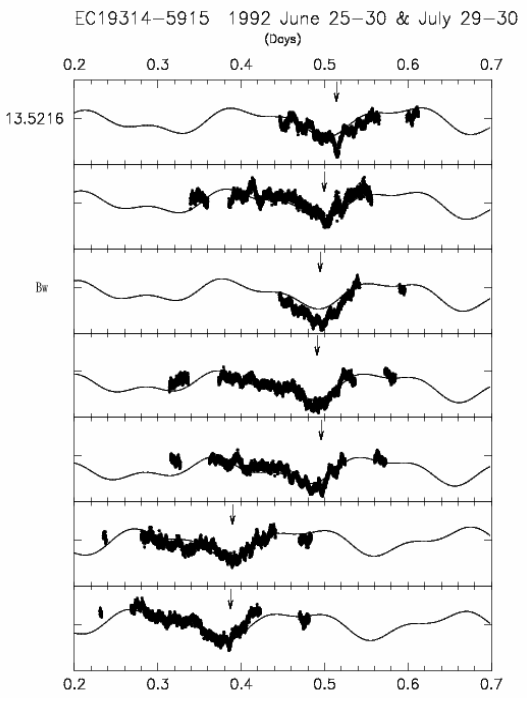

Fig. 2 Light variations out of eclipses.

long-term variation for the system brightness is found. The peak of 0.002046 mHz ($5^d.6569$) is the dominant low frequency in the range 0-0.02 mHz (arrowed in Fig. 3). The solid line shown in Fig. 4 is the least-squares with the frequency fitted to the data of June 25-30 and July 29-30.

In CVs, precession period is about 10-35 times of orbital period for the range $0.1 < q < 1$ (Warner 1995). The presence of the period ~$28.56P_{orb}$ may imply an existence of a tilted disc that precesses under the influence of the gravitational fields of other components.

Combining the precession, hump and orbital modulations, sinusoids of these frequencies were fitted to the data of Fig. 2 by least-squares. The curve (Fig. 2) fits the data reasonably well and may explain why the eclipse profile varies in successive eclipses. Smooth ingress occurs in "catch-up mode" that eclipse begins before maximum of the hump - the brightest region moves into observer's sight first. Steep ingress happens

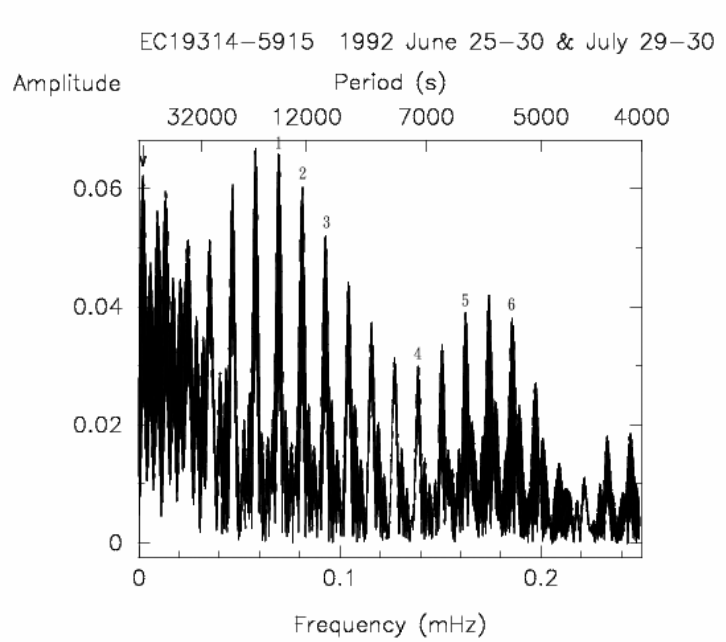

Fig. 3 Fourier amplitude spectrum for out of eclipses. The numbers 1, 2, 3, 4, 5 and 6 mark the periods 3.9856, 3.4010, 2.9775, 1.9933, 1.7008 and 1.4890 h, respectively.

Table 3. Times of Minimum Light for Out of Eclipses

T_{min} (HJD)	Orbital Phase	Hump Phase[*1]	Hump Phase[*2]	Hump Phase[*3]	Phase corresponding to P_{pr}
8799.515003	0.67	0.0	0.0	0.0	0.0
8800.500663	0.65	0.94	0.96	0.94	0.174
8801.495758	0.67	0.93	0.98	0.97	0.350
8802.492237	0.70	0.93	0.01	0.0	0.526
8803.497629	0.78	0.98	0.10	0.10	0.704
8833.390096	0.69	0.99	0.04	0.05	5.988
8834.386224	0.71	0.99	0.07	0.08	6.164

Footnote: [*1] the phases corresponding to the period 3.9856h
[*2] the phases corresponding to the period 3.4010h
[*3] the phases corresponding to the period 2.9775h

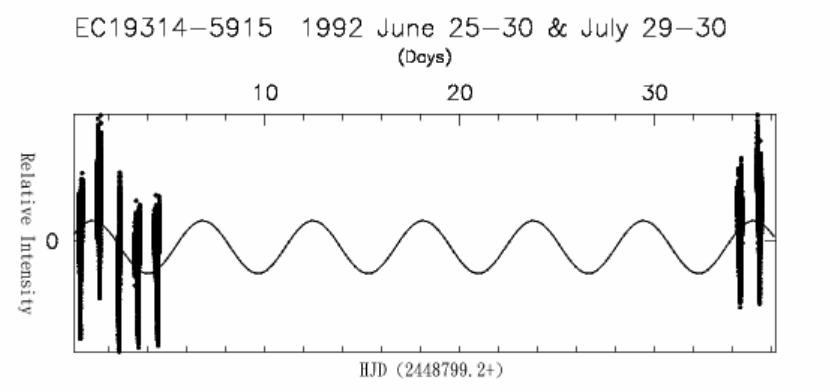

Fig. 4. Long-term light variation

in "over-take mode" that the brightest region is occulted by the secondary before get into observer's sight.

3.3 Orbital Modulation and Quasi-Periodic Oscillations

The HSP data were binned into orbital phase using the photometric ephemeris obtained in the above and are shown in Fig. 5. The mean orbital light curve (Fig. 5) exhibits a significant orbital modulation with a peak-to-peak amplitude of ~30%. This orbital modulation may rise from the asymmetric distribution in brightness on the disc. In order to search for other possible variations, separation of the orbital modulation from the light curve was attempted. First, an amplitude spectrum (Fig. 6) was calculated for the "hump" data (data of Fig. 5 excluding the eclipses) and reveals three most prominent peaks at frequencies 0.05842697, 0.108, and 0.174 mHz. To derive the best fit for the hump, three sinusoids of initial frequencies equal to those of the highest peak in the amplitude spectrum was fitted to the "hump" data by non-linear least-squares and gave best fitted frequency (f), amplitude (A) and phase (ϕ) for the sinusoids:

f (mHz)	A	ϕ
0.05842779	0.07744	-0.04922
0.11688735	0.03712	-4.27045
0.17529573	0.01893	-1.75510

Second, these three sinusoids were used to construct the fitted curve for the hump (Fig. 7) and then the fitted curve was subtracted from the data of Fig. 5. This yields an almost flat light curve out of eclipses (Fig. 8), i.e. the trend of the asymmetric brightness distribution is removed.

Fourier amplitude spectrum (Fig. 9) was calculated for the data out of eclipse and

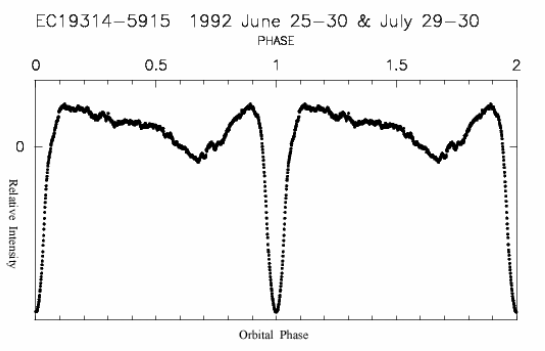

Fig. 5 The mean light curve - all the HSP data binned in orbital phase

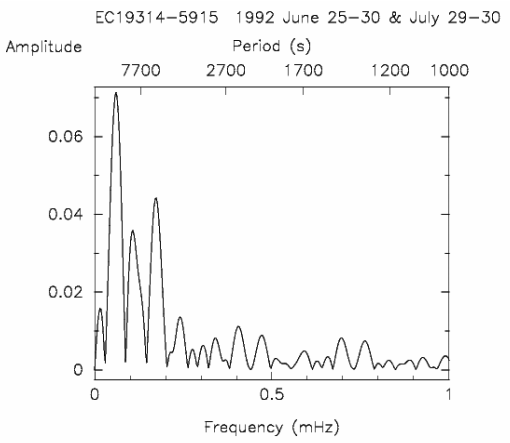

Fig. 6 Fourier amplitude spectrum calculated for the "hump" data.

reveal no evidence for any periodic behaviour with amplitudes greater than 0.1% at frequencies≧ 3 mHz. Two highest peaks correspond to the humps in the light curve. The rest of the spectrum show peaks of ≧ 0.2% spread over the frequency range 1.0-3.0 mHz. Note that the power in quasi-periodic oscillations (QPOs) is spread over a range of frequencies. A sinusoid of the frequency of these peaks near 1.8 mHz was fitted to the corresponding data of Fig. 8 by least squares. The resulting period is 582s (1.719 mHz). The arrows in Fig. 10 indicate the times of maximum light corresponding to the period fitted to the run. The calculated times of maximum light seem to match the observed times at the beginning and in the middle of the run. There is poor coherence at the end of the run.

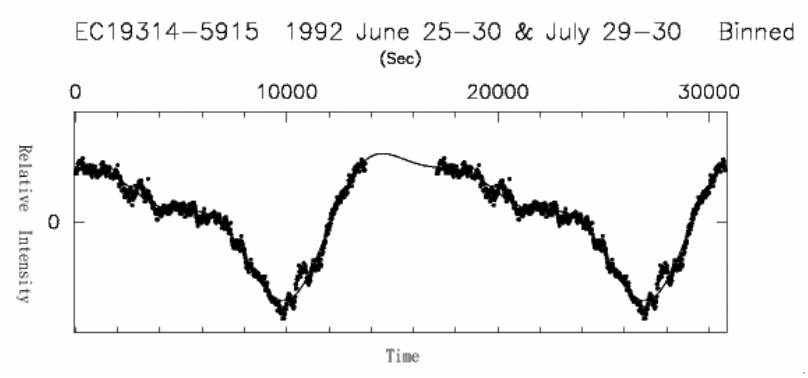

Fig. 7 The solid curve is the best fit to the hump.

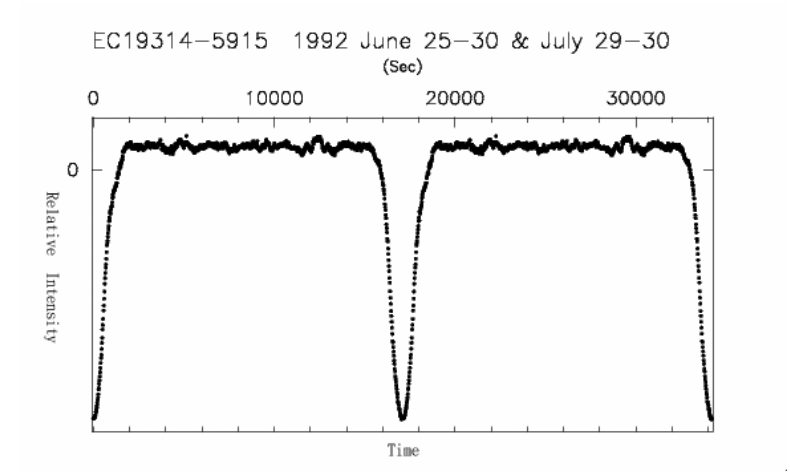

Fig. 8 The mean light curve after hump-removed.

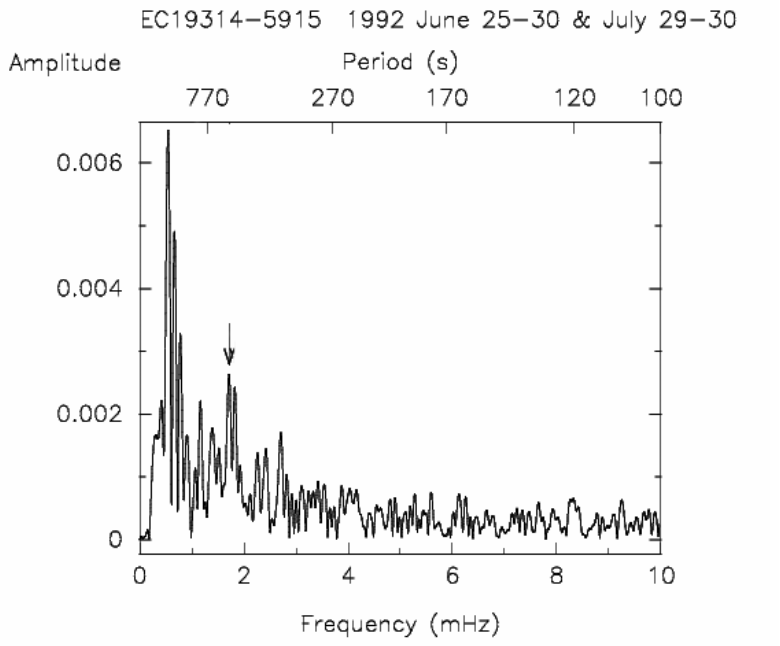

Fig. 9 Fourier amplitude spectrum of the data outside the eclipses. The arrow marks the period of the QPOs.

QPOs are low amplitude, poor coherent light variation with periods in the range of ~50-1000s. The excitation mechanism might arise from three radii in an accretion disc (Warner & Woudt 2002). Assume the oscillations occur at the inner edge of the disc, near radius r_0, the Keplerian period as a function of the orbital period is given as follows (Warner & Woudt 2002):

$$\frac{P_k(r_{\min})}{P_{orb}} = 0.0107 \cdot q^{-0.7}(1+q)^{\frac{1}{2}} \qquad (1)$$

Let's assume the QPO period is comparable to the Keplerian period at the inner edge of the disc. Substituting the QPO period and the orbital period into Eq.(1), the mass ratio ($q=M_2/M_1$) of the system is estimated to be 0.22111.Warner (1995) derived a mean empirical mass-period relationship for the secondary in CVs.

$$M_2 = 0.065 \cdot P_{orb}^{\frac{5}{4}} \qquad (2)$$

where P_{orb} is in hours. The relationship is valid for P_{orb} in the range $1.3 \le P_{orb} \le 9$ h.

Using Eq.(2), the mass of the secondary is estimated to be 0.456 $M_\odot$. If the mass ratio is 0.22111, then the mass of the white dwarf exceeds the Chandrasekhar limit. This estimate implies that the primary is very likely a high-mass white dwarf if the QPOs did occur at the inner edge of the disc.

4. Synthetic Analysis of Light Curves

Warner & Nather (1971) and Smak (1971) independently proposed a same model for CVs that the light comes from three sources: the primary, the secondary that overflows its Roche-lobe and the accretion disc with a bright spot at the outer edge. Based on the above model, a light-curve synthesis programme was developed to derive the geometric and physical parameters such as the dimensions of the components and the temperatures of the components. The synthesis programme adjusted the parameters of the model to reconstruct the light curves that optimized the fit of the reproduced curves to the observed light curves. A similar method was used in the studies of eclipses such as in RW Tri (Frank & King 1981), UX UMa and U Gem (Frank et al. 1981), and HT Cas (Zhang, Robinson & Nather 1986). In the above studies, the light curves of NLs were well fitted by the eclipse of an optically thick, steady state accretion disc but those of DN were not well fitted.

Few assumptions were made for the programming: (a) the orbit is circular and the rotation of the stars is synchronous; (b) both stars are spherical; (c) the accretion disc is

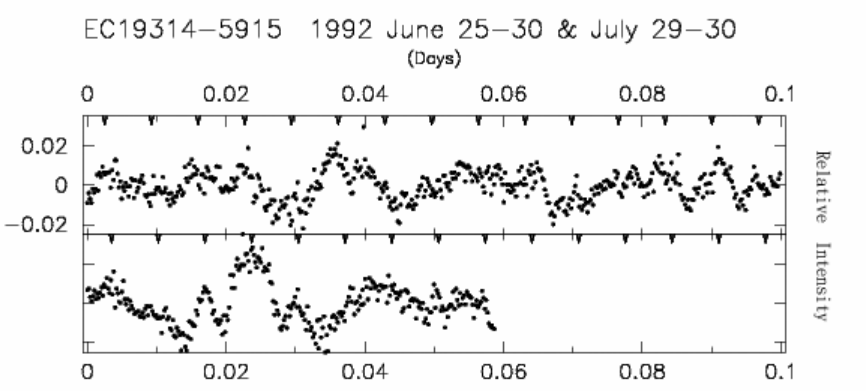

Fig. 10 Light variation out of eclipse with hump-removed. The arrows indicate the calculated times of maximum light.

circular, optically thick, and lying in the orbital plane; (d) both stars behave as blackbodies. The first step in the fitting procedure is to calculate the eclipse geometry for the disc and the primary. Horne's (1985) algorithm was adopted: the surface of the disc is divided into a Cartesian grid of N×N discrete elements. The total accretion disc flux at a given orbital phase can be calculated by summing contributions from all visible elements:

$$f_{disc}(\phi) = A_i \sum_{i=1}^{N^2} I(i) \cdot V(i,\phi) \qquad (3)$$

The A_i is the area of the element *i*, *I*(*i*) is the intensity emitted by the surface element *I* and *V*(*i*, ϕ) represents the visibility of the element at phase ϕ. If the centre of a surface element is visible, $V(i,\phi)$ is set a value of 1. Otherwise, it is assigned to be 0. To decide whether a surface element is visible at a given phase, both the disc and the secondary were first projected onto the plane of the sky. An occultation happens if the projected disc of the secondary obscures an element on the projected accretion disc along the line of sight. The U-hypothesis (Tsesevich 1973) is used to calculate the fraction of the surface of the primary occulted by the secondary at a given phase. The total flux of the primary at a given phase is calculated from the following:

$$f_{wd}(\phi) = f_0 \cdot [1 - \beta(\phi)] \qquad (4)$$

where f_0 is the primary's flux out of eclipse and $\beta(\phi)$ is the ratio of the eclipse area.

The next, a synthetic light curve can be obtained by summing the contributions from the components: the primary, the secondary and the accretion disc. The contribution of other sources in the system, such as bright spot and G dwarf, is neglected because the asymmetrical distribution is removed from the observed light curve (see Fig. 8) and the 23 per cent contribution of G dwarf is deducted from the light curve.

To start the fitting procedure, we need to determine the ranges of few parameters, which are discussed as follows:

(a) Buckley et al. (1992) suggested that the mass of the white dwarf is possibly in the range of $1.4M_\odot \le M_1 \le 0.5M_\odot$ and the mass ratio of the system is less than unity.

(b) If the mass ratio is less than unity, the M_2 falls in between 0.2 $M_\odot$ and 0.5 $M_\odot$ for a red dwarf.

(c) The radius of the primary is estimated using the mass-radius relationship for non-rotating helium white dwarf (Warner 1995).

$$R_1 = 0.779 \cdot [(\frac{M_1}{M_{ch}})^{-\frac{2}{3}} - (\frac{M_1}{M_{ch}})^{\frac{2}{3}}] \times 10^9 cm \qquad (5)$$

where M_{ch} the Chandrasekhar limit, 1.44 $M_\odot$.

(d) Because the secondary fills its Roche lobe, its radius is considered equivalent to the volume radius R_{L2} of the Roche lobe.

$$\frac{R_2}{a} = \frac{0.49 \cdot q^{\frac{2}{3}}}{0.6 \cdot q^{\frac{2}{3}} + \ln(1 + q^{\frac{1}{3}})} \qquad (6)$$

where *a* is the orbital separation. Eq.(6) was derived by Eggleton (1983) and accurate to better than 1%.

(e) The mass flow from the secondary goes through the inner Lagrangian point and then forms an accretion disc around the primary. Thus the inner edge of the disc is beyond the surface of the primary and the outer edge of the disc is lying inside the Roche lobe of the primary.

(f) In some CVs, the effective temperatures (T_1) were deduced for the white dwarfs. T_1 shows a range between 10,000K and 50,000K.

(g) Since the secondary is likely a late-type dwarf, we assume the effective temperature (T_2) falls in the range,

2500-4500K.

(h) Assume the surface temperature distribution follows an optically thick, steady state accretion disc. The temperature at a position *r* in the disc is (Warner 1995)

$$T_d(r) = T_* \cdot (\frac{r}{R_1})^{-\frac{3}{4}} \cdot [1-(\frac{R_1}{r})^{\frac{1}{2}}]^{\frac{1}{4}} \quad (7)$$

where

$T_* = 4.10\times10^4 \cdot (\frac{R_1}{10^9})^{-\frac{3}{4}} \cdot M_1^{\frac{1}{4}} \cdot (\frac{\dot{M}}{10^{16}})^{\frac{1}{4}}$,

$\dot{M}$ is the accretion rate, about 10^{16}-10^{18} gm · s^{-1}.

(i) The last parameter required is the inclination *i*, which is assumed to be 70-90°, an empirical range for the eclipsing CVs.

A computation for a single set of parameters was tested on a Linux platform installed on a PC equipped with a PII 350MHz CPU and 392 MB RAM. It took about 4 minutes to complete the calculation. A thorough numerical simulation requires calculating more than 5 millions combinations, which take too much time. Thus the calculations were conducted with wider parameter-steps (Table 4). After the best fits were obtained, parameter sets in those fits were calculated again but with finer steps (half the previous width).

Table 4. Fitting Parameters

Parameter	Range	Step
M_1	0.5-1.4$M_\odot$	0.1 $M_\odot$
M_2	0.2-0.5$M_\odot$	0.1 $M_\odot$
T_1	10000-50000K	10000K
T_2	2500-4500K	1000K
i	70-90°	5°
$\dot{M}$	10^{16},10^{17},10^{18} gm · s^{-1}	

5. Results and Discussion

Using the method mentioned in the previous section, the calculations for the fitting parameters of Table 4 reveal no fit with a standard deviation less than 0.0277. Although no satisfactory solutions were obtained, the best fits ($0.0277 < \sigma < 0.0299$) give

M_1	1.2-1.4$M_\odot$	M_2	0.3-0.4$M_\odot$
R_1	0.006-0.002$R_\odot$	R_2	0.439-0.460$R_\odot$
T_1	25000-50000K	T_2	3500K
T_{out}	1850-3400K		
R_{in}/a	0.1266-0.1283	R_{out}/a	0.2524-0.5657
a	1.1425-1.2027×10^{11} cm		
i	81-90°°		
$\dot{M}$	10^{16} gm · s^{-1}		

The larger deviation for the light-curve fit may be due to the assumption of the radiation at monochromatic wavelength 4400Å. In fact, the HSP was observed in white light, a "broad B-band", which differs from the Johnson B-band.

The results presented here are preliminary. In order to obtain more precise solutions for the system, it requires not only further calculations with parameters in wider ranges with fine steps but also HSP in multiple bandpasses (UBVRI) for study of eclipses/QPOs and determination of temperatures. In addition, time-resolved spectroscopy is needed for the estimate of the mass ratio of the system.

REFERENCES

Buckley D.A.H., O'Donoghue D., Kilkenny D., Stobie R.S., Remillard R.A., 1992, *MNRAS*, 258, 285

Eggleton P.P., 1983, ApJ, 268, 368

Frank J., King A.R., 1981, *MNRAS*, 195, 227

Frank J., King A.R., Sherrington M.R., Jameson R.F., Axon D.J., 1981, *MNRAS*, 195, 505

Ghedini S., 1982, Software for Photometric Astronomy, Willmann-Bell Inc.
Smak J., 1971, *Acta Astr*, 21, 15
Tsesevich V.P., 1973, in Tsesevich V.P. ed., Eclipsing Variable Stars, Israel Program for Scientific Translations Ltd., Ch2
Warner B., 1995, Cataclysmic Variable Stars, Cambridge University Press
Warner B., Nather R.E., 1971, *MNRAS*, 152, 219
Warner B., Woudt P.A., 2002, *MNRAS*, 335, 84
Zhang E.-H., Robinson E.L., Nather R.E., 1986, *ApJ*, 305, 74